

Cite this article as: Ming Yue, You Guoqiang, Peng Lizhen, et al. Study on Adsorption Oxidation of Mg_2Ca and $\alpha\text{-Mg}$ in Mg-Ca Alloy by DFT[J]. Rare Metal Materials and Engineering, 2022, 51(10): 3563-3573.

ARTICLE

Study on Adsorption Oxidation of Mg_2Ca and $\alpha\text{-Mg}$ in Mg-Ca Alloy by DFT

Ming Yue¹, You Guoqiang^{1,2}, Peng Lizhen¹, Zhang Jun³, Zeng Wen¹, Zhao Jianhua^{1,2}

¹ School of Materials Science and Engineering, Chongqing University, Chongqing 400044, China; ² National Engineering Research Center for Magnesium Alloys, Chongqing University, Chongqing 400030, China; ³ Technical University of Munich, Munich 80333, Germany

Abstract: The oxidation of $\alpha\text{-Mg}$ and Mg_2Ca in Mg-Ca alloy was studied by calculating the adsorption process of O_2 on $\alpha\text{-Mg}$ (0001) and Mg_2Ca (0001) based on density functional theory (DFT), and the adsorption process and oxidation mechanism were investigated. Results show that during the adsorption, O_2 has a strong interaction with $\alpha\text{-Mg}$ and Mg_2Ca . The interactions are chemisorption due to the excellent E_{ad} values, but the adsorption structures of Mg_2Ca are not as stable as that of $\alpha\text{-Mg}$. During the oxidation, O_2 reacts with Ca and Mg atoms in $\alpha\text{-Mg}$ and Mg_2Ca to form Mg-Ca-O oxide film, hence improving the oxidation resistance of Mg-Ca alloy. Since the adsorption structure of Mg_2Ca is not as stable as that of $\alpha\text{-Mg}$, the oxide film formed by Mg_2Ca shows weaker protective effect on the substrate than that formed by $\alpha\text{-Mg}$.

Key words: Mg_2Ca ; $\alpha\text{-Mg}$; oxidation; density function theory

Owing to the excellent properties, such as low density, admirable specific strength and specific stiffness, strong electromagnetic shielding ability and environment friendly, magnesium alloys show great potential to be applied as structure materials^[1-5]. Nevertheless, Mg shows high affinity to oxygen, especially at high temperatures^[6,7]. The MgO film shows poor protection to the substrate, resulting in severe oxidation, even burning, which seriously restricts the promotion and application of Mg alloys^[8,9]. Reports indicate that alloying can significantly improve the oxidation resistance of Mg ^[10-13]. Mg-Ca alloy, free of expensive rare-earth elements, has drawn much attention due to the favorable properties^[14,15].

Many researches have illuminated that Ca can remarkably enhance the oxidation resistance of Mg. Lee et al^[16,17] studied the influence of CaO on oxidation resistance of AZ31 and AZ61. Results demonstrated that the oxidation resistance is significantly improved by the addition of CaO , which is attributed to CaO oxide film formed on the surface. Cheng et al^[18] verified that a CaO/MgO composite oxide film is formed on the surface of AZ80 by the addition of Ca, which is ascribed to the dissolved Ca in $\alpha\text{-Mg}$. Paridari et al^[19] found

that with the addition of 2wt% Ca, the Mg melt can be exposed to air for 40 min at 700 °C without any protection, which is ascribed to the dense CaO oxide film on the surface.

Mg_2Ca and $\alpha\text{-Mg}$ are the common phases in Mg-Ca alloy. However, reports have insisted that the dissolved Ca in $\alpha\text{-Mg}$ contributes to the formation of CaO oxide film, while the high-temperature stable phase Mg_2Ca is beneficial to the improvement of oxidation resistance by raising the melting point of the substrate^[20,21]. Therefore, the oxidation mechanism of Mg_2Ca and $\alpha\text{-Mg}$ remains unclear until now. In this study, the first principle was applied to analyze the adsorption of O_2 on Mg_2Ca and $\alpha\text{-Mg}$ from the atomic level, in order to reveal the role of Mg_2Ca and $\alpha\text{-Mg}$ in oxidation. Although it is difficult to verify based on experiment, this research draws on a large number of researches, which shows super adaptability. The obtained results will fill the gap of the specific effect of Mg_2Ca and $\alpha\text{-Mg}$ on the oxidation of Mg-Ca alloy from atomic level.

1 Models and Calculation

Ca is dissolved in $\alpha\text{-Mg}$ in the form of replacement solid solution^[22]. To avoid the interaction between adjacent cells, a

Received date: October 13, 2021

Foundation item: Guangdong Province Key Field R&D Program Project (2020B010186002); National Natural Science Foundation of China (U2037601); Dongguan Key Technology Key Project (2019622134013)

Corresponding author: You Guoqiang, Associate Professor, Chongqing University, Chongqing 400044, P. R. China, Tel: 0086-23-65112626, E-mail: yqg@cqu.edu.cn

Copyright © 2022, Northwest Institute for Nonferrous Metal Research. Published by Science Press. All rights reserved.

4×4 Mg supercell with periodic boundary condition (1.271 nm×1.271 nm) and a 2×2 Mg₂Ca supercell with periodic boundary condition (1.242 nm×1.242 nm) were applied. As far as adsorption, a six thickness supercell was established to carry out the O₂ adsorption process, with a vacuum region of 10 nm to protest the interaction between adjacent units. The close-packed lattice plane (0001) with the lowest surface energy was applied as the adsorption surface^[23]. The bond length of O₂ was 0.1225 nm, which was 1.24% higher than the experimental value of 0.1210 nm^[24]. For comparison, the Mg adsorption process was also calculated. The adsorption sites of Mg and Mg₂Ca are shown in Fig.1 and Fig.2. For α-Mg with substitution adsorption in Fig.1, the central Mg atom (site ④) was replaced by a Ca atom.

The density functional theory (DFT) calculations were conducted in Vienna Ab-initio Simulation Package (VASP)^[25]. Perdew-Burke-Ernzerhof (PBE) function with generalized gradient approximation (GGA) was employed to calculate the electronic structure and involved terms^[26-28]. The Brillouin zone k-point sampling was set in 2×2×1 Monkhorst-Pack mesh^[29]. The cutoff energy for the plane wave basis set was set to 450 eV. The convergence criteria for energy and force were set to 10⁻⁵ eV and 0.1 eV/nm, respectively. Note that GGA-PBE does not contain the van der Waals force in the system, so the DFT-D (Grimme) algorithm was used to optimize the geometry of the adsorption model^[30-32].

The adsorption energy (E_{ad}) was defined as follows^[33,34]:

$$E_{ad} = E_{\text{substrate/gas molecule}} - E_{\text{substrate}} - E_{\text{gas molecule}} \quad (1)$$

where $E_{\text{substrate/gas molecule}}$, $E_{\text{substrate}}$ and $E_{\text{gas molecule}}$ refer to the total

energies of the system after adsorption, substrate and optimized gas molecule, respectively. Based on this definition, a negative E_{ad} refers to an exothermic and energy-favorable process, and the structure with the lowest E_{ad} will be the most stable.

2 Results and Discussion

2.1 Adsorption CPK model

In order to better understand the distribution of atoms after adsorption, the Corey-Pauling-Koltun (CPK) model is used, as shown in Fig.3 and Fig.4. Due to different adsorption sites, the initial positions of O atoms are different. Hence, the distances and interactions of Mg-O and Ca-O are different, resulting in different adsorption structures. Besides, O atoms tend to migrate to Ca atoms. That is, O tends to react with Ca rather than Mg.

2.2 Adsorption analysis

The adsorption energy of α-Mg and Mg₂Ca adsorption system is shown in Fig.5 and Fig.6. These results reveal that the adsorption can be identified as strong chemisorption due to the adsorption values lower than -0.8 eV^[35,36].

In Mg adsorption systems, adsorption site ② shows the most stable adsorption structure. While in α-Mg adsorption systems, adsorption site ④ shows the most stable adsorption structure. Comparing the adsorption energy of Mg and α-Mg, it can be seen that the adsorption energy of α-Mg is greater, indicating that the adsorption structure is more stable. In Mg₂Ca adsorption systems, adsorption site ⑤ shows the most stable adsorption structure^[37,38].

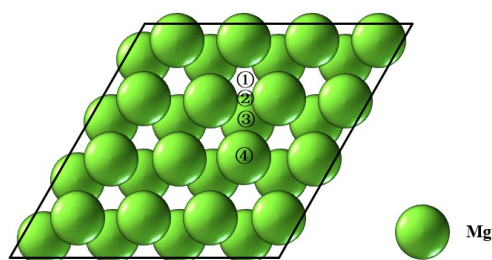


Fig.1 Adsorption sites of the Mg (0001) lattice surface (① fcc hollow, ② bridge, ③ hcp hollow, and ④ top)

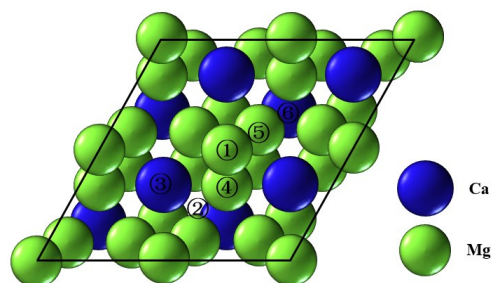


Fig.2 Adsorption sites on Mg₂Ca (0001) lattice surface (① Mg top, ② Mg-Mg bridge, ③ Ca top, ④ Ca-Ca bridge, ⑤ Ca-Ca bridge, and ⑥ hollow)

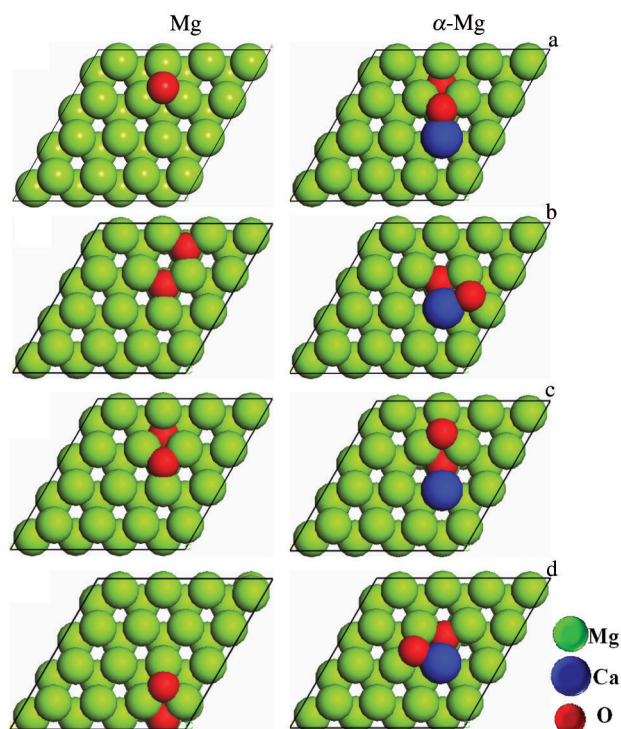


Fig.3 CPK models of Mg and α-Mg adsorption systems: (a) site ①, (b) site ②, (c) site ③, and (d) site ④

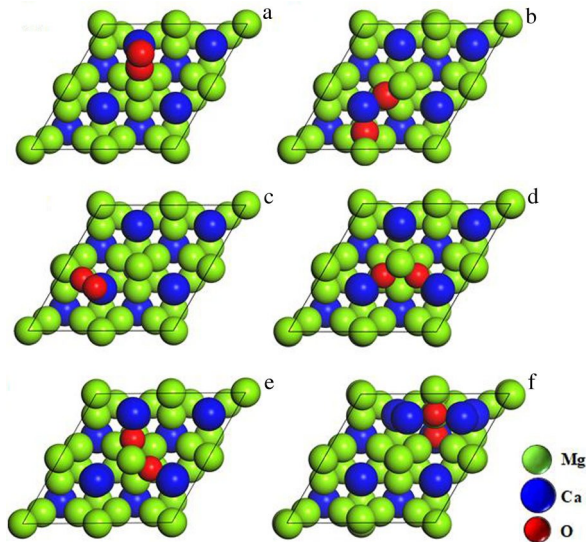


Fig.4 CPK models of Mg_2Ca adsorption systems: (a) site ①, (b) site ②, (c) site ③, (d) site ④, (e) site ⑤, and (f) site ⑥

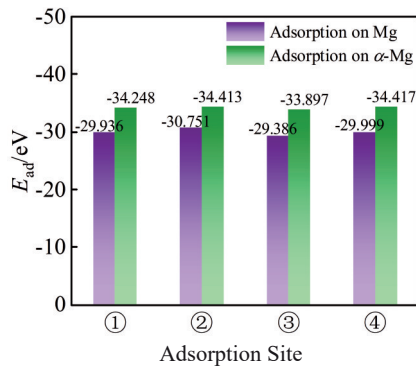


Fig.5 E_{ad} values of Mg and α -Mg adsorption systems

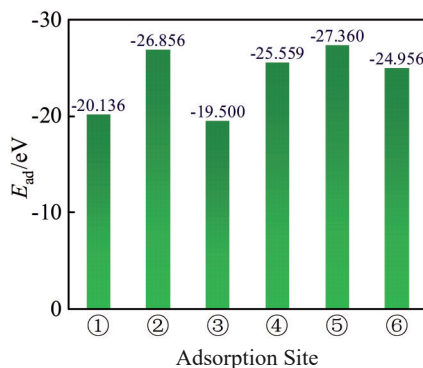


Fig.6 E_{ad} values of Mg_2Ca adsorption systems

The obtained adsorption configurations and electron density are shown in Fig.7~Fig.9, where the isosurface value is set to $0.2 \times 10^3 \text{ e/nm}^3$ in the electron density. The distortion of the bonds during the adsorption process and electron cloud overlapped in the electron density can be observed directly, which indicate the strong interaction in these adsorption

systems. For a better description, the O1 atom refers to the O atom that diffuses deeply in the substrate, and O2 atom refers to the O atom that diffuses shallowly in the substrate.

For Mg adsorption systems, as shown in Fig.7, it can be seen directly that the O-O bond undergoes breakage after adsorption, because the distance between the two atoms is larger than the O-O bond length. Mg atoms react with O and leave their initial positions, that is, Mg atoms diffuse outward to a certain degree to react with O atom diffused inward. In Fig.7a on site ①, the O-O suffers breakage because the O-O distance changes from 0.1225 nm to 0.2668 nm. O1 atom is bonded with three Mg atoms on the next layer, and O2 atom is bonded with three Mg atoms on the surface. From the adsorption configuration on site ② depicted in Fig.7b, it is found that the both O atoms are bonded with three Mg atoms on the surface with the similar bond lengths. For adsorption on site ③, as described in Fig.7c, O1 atom is bonded with two Mg atoms on the next layer with the same bond length, and O2 atom is bonded with 3 Mg atoms on the surface. As shown in Fig.7d on site ④, O-O bond is broken and O atoms are trapped by Mg atoms nearby.

As shown in Fig.8, O atoms are released from the gas molecular and trapped by the atoms nearby, because the distance between the two atoms is larger than the O-O bond length. Mg and Ca atoms reacting with O leave their initial positions. That is, Mg and Ca atoms diffuse outward to a certain degree to react with O atoms diffused inward. Besides, the diffused distance of Ca atom outward is greater than that of Mg atom, indicating that the affinity of Ca and O is greater than that of Mg and O. As shown in Fig.8a, the adsorption of O_2 on α -Mg at position ① is depicted. O atoms are captured by the Mg and Ca atoms nearby. The O1 atom is bonded with two Mg atoms with the same bond length, while O2 atom is bonded with two Mg atoms and one Ca atom. In Fig.8b, the adsorption at site ② is depicted. The two O atoms are both bonded with one Ca atom and two Mg atoms. At site ③ shown in Fig.8c, only O1 atom is bonded with Ca. When it comes to the site ④ in Fig.8d, the adsorption structure is similar to that at site ②, and the two O atoms are both bonded with one Ca atom and two Mg atoms.

As we can see, for Mg_2Ca adsorption systems, the O-O bond remains connected at site ① and ③. However, for other adsorption sites, the O-O bonds undergo breakage after adsorption, because the distance between the two atoms is larger than the O-O bond length. It can be implied that the adsorption energies of site ① and ③ are lower than those of site ②, ④, ⑤ and ⑥, which is consistent with the E_{ad} values. It also implies that the adsorption structures of site ① and ③ are more unstable than those of other sites. In Fig.9a on site ①, the O-O bond keeps connected. O1 atom is bonded with one Mg atom and one Ca atom, and O2 atom is bonded with the same Ca atom. For adsorption on site ③, as described in Fig.9c, the adsorption structure is similar to the adsorption structure on site ①. From the adsorption configurations on site ②, ④ and ⑤ depicted in Fig.9b, 9d and 9e, O atoms diffuse inwards with almost the same distance, and are all

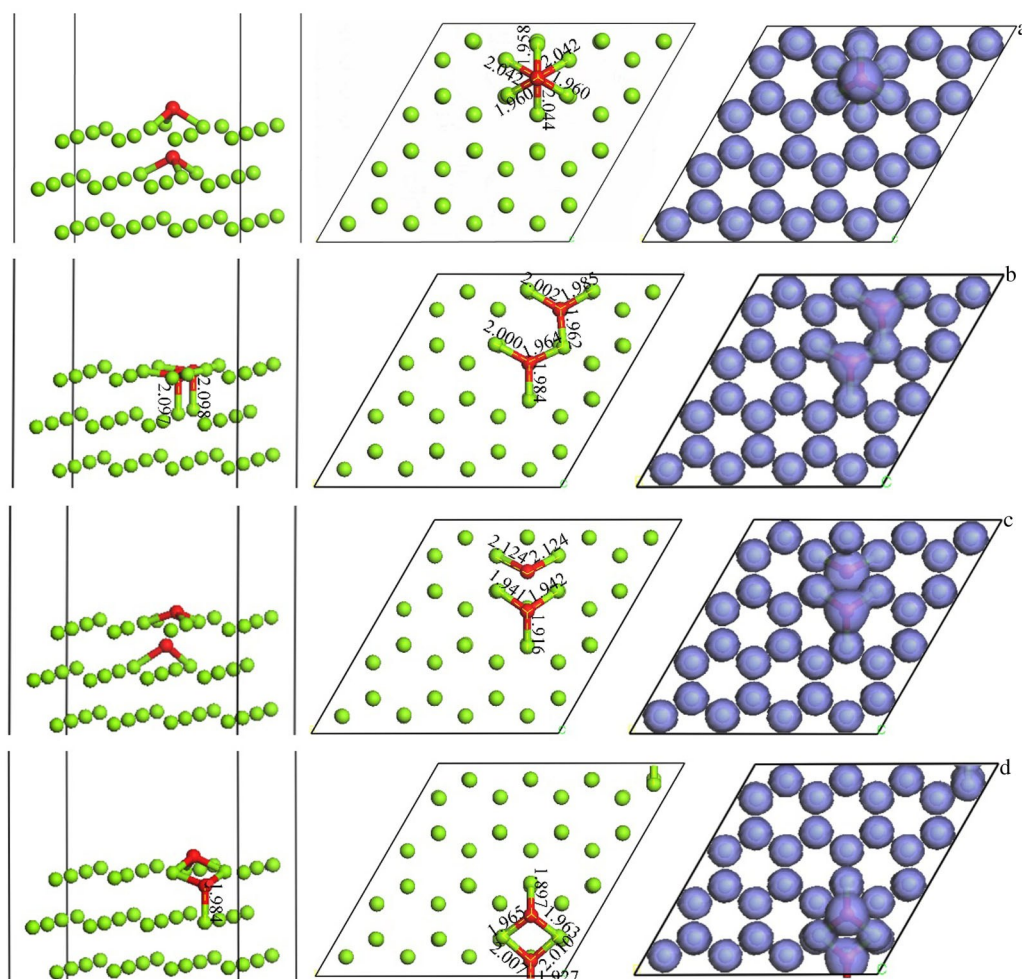


Fig.7 Adsorption configurations and parameters for adsorption system of Mg: (a) site ①, (b) site ②, (c) site ③, and (d) site ④

bonded with the same number of Mg atoms and one Ca atom, with the similar Mg-O bonds and Ca-O bond lengths. As shown in Fig. 9f on site ⑥, O atoms diffuse inwards with different distance. O1 atom is bonded with three Mg atoms and one Ca atom, and O2 atom is bonded with two Mg atoms and two Ca atoms.

Overall, O_2 shows strong absorbing ability toward Mg, α -Mg and Mg_2Ca , and the adsorption systems can be assumed as chemisorption due to the excellent E_{ad} values, and the E_{ad} values are comparably higher than that of other adsorption systems reported before. This is due to the fact that Mg is easy to oxidize, and the oxidation process emits a lot of heat. After adsorption, Mg-O is formed on Mg, and Mg-Ca-O is formed on α -Mg and Mg_2Ca . Combined with the E_{ad} results, the Mg-Ca-O formed on α -Mg is more stable than the Mg-O formed on Mg.

2.3 Electronic structure for different systems

To further reveal the electronic structure of adsorption systems, the density of states (DOS) and electron density difference were investigated. The density of state distributions is described in Fig. 10~Fig. 12. The density of state distributions of the intrinsic substrate and the one after adsorption are shown in the same scheme for better comparison. The partial

density of state distributions is also plotted for better comprehending the interactions simultaneously. For all the adsorption systems, the peaks after adsorption are different for isolated systems, which can be attributed to the charge transfer between the adsorbent surface and the adsorbed molecule. Besides, the overlapping areas indicate the high hybridization between atoms.

Fig. 10 portrays the DOS distributions of Mg adsorption systems. O atoms undergo hybridization with Mg atoms in similar ways on site ① and ④, due to the overlapping areas between O 1p, O 2s, O 2p and Mg s, Mg p, as shown in Fig. 10a and 10d. On the position ③ described in Fig. 10c, the hybridization can be confirmed by the overlapping area between O 1s, O 1p, O 2s, O 2p and Mg s, Mg p. Unlike DOS distributions above, the two O atoms show almost the same DOS distributions on site ②, as shown in Fig. 10b, and the orbits are overlapped with Mg s and Mg p, also illustrating the hybridization.

Fig. 11 depicts the density of states distribution of α -Mg adsorption system. The similar adsorption structures on adsorption sites ② and ④ lead to the similar distribution. For all adsorption sites, the overlapping regions of the density of states between O1 s, O1 p, O2 s, O2 p and Mg s and Mg p

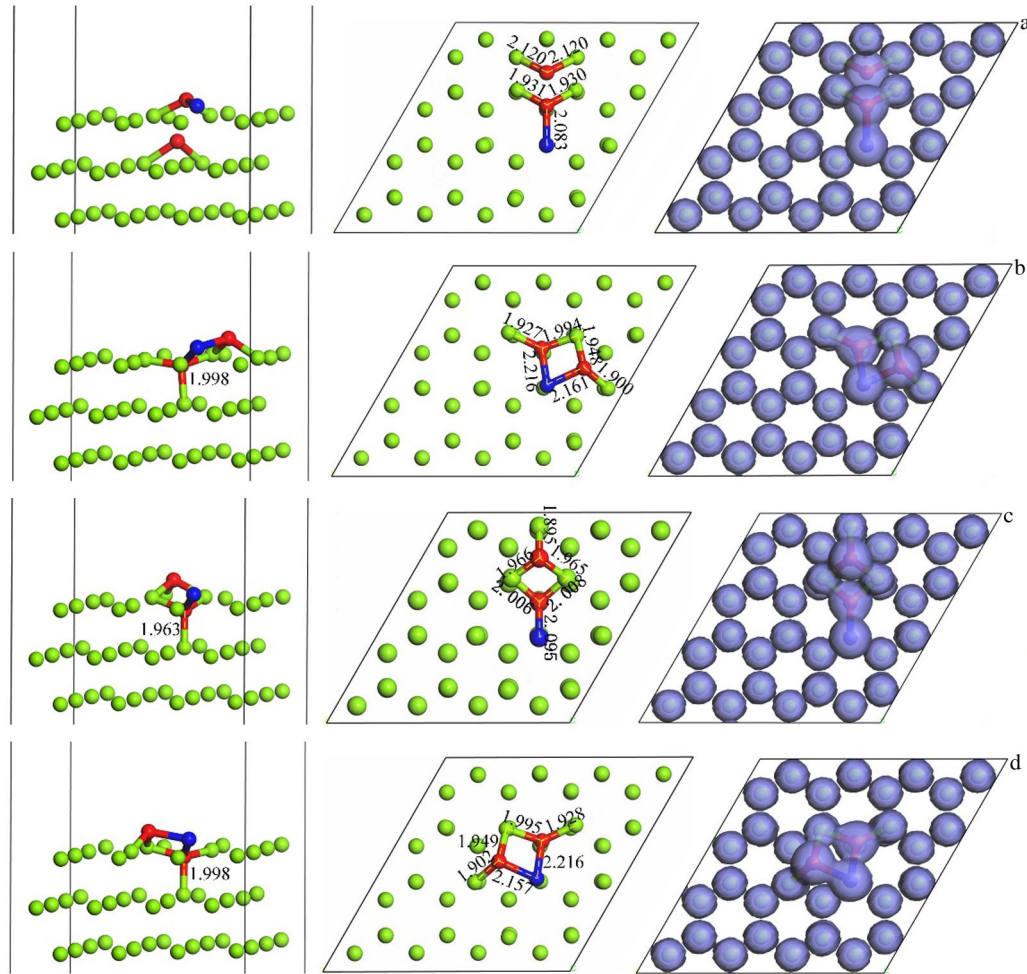


Fig.8 Adsorption configurations and parameters for adsorption system of α -Mg: (a) site ①, (b) site ②, (c) site ③, and (d) site ④

indicate the strong hybridization between them.

Fig.12 describes the density of states distribution of Mg_2Ca adsorption systems. As analyzed above, site ① and ③ possess the similar adsorption structure, which can be further verified in the density of states, as shown in Fig.12a and 12c. The two O atoms on site ②, ④ and ⑤ are bonded with the same atoms in one adsorption system. Hence, the distributions of the two O atoms in one adsorption system are similar.

It can be seen directly that the distributions on site ⑥ is similar to that on site ⑤. This is due to the similar adsorption structures between O1 atom on site ⑥ and O atoms on site ⑤. Overall, similar adsorption structures have similar distributions, and the overlapping areas between atomic orbitals indicate strong hybridization between atoms.

The charge-transferring path during the adsorption process can be confirmed by the electron density difference, as displayed in Fig.13~Fig.15. The blue and yellow areas refer to electron accumulation and depletion, respectively. The isosurface is set to 30 e/nm^3 . The Hirshfeld analysis was also conducted to illustrate the charge transfer between the O_2 and substrate surface. A positive value represents that the atom is an electron donor while a negative value indicates the electron-accepting behavior for the target atom^[39]. The

Hirshfeld charge of O atoms and bonding Mg and Ca atoms is tabulated in Table 1.

For Mg adsorption systems, the electron accumulation is mainly localized at the O atoms while electron depletion is mainly localized at the Mg atoms nearby. Combined with the Hirshfeld charge, O atoms obtain electrons of 0.894, 0.868, 0.860, 0.931 e and Mg atoms nearby lose electrons. For α -Mg adsorption systems, the electron accumulation is mainly localized at the O atoms while electron depletion is mainly localized at the Mg atoms nearby. However, electron accumulation and depletion are both localized at the Ca atom, and electron depletion mainly exists along the Ca-O bond. The result is consistent with the Hirshfeld charge, in which the O atoms obtain electrons of 0.895, 0.965, 0.957, 0.956 e, and Mg atoms lose electrons. Besides, Hirshfeld charge indicates that Ca loses electrons finally. Combined with the Hirshfeld charge results of these systems, it can be seen that α -Mg donates more electrons to O_2 than Mg, demonstrating the stronger electrostatic attraction in α -Mg systems.

As displayed in Fig.15, for Mg_2Ca adsorption systems, the electron accumulation is mainly localized at the O atoms while electron depletion is mainly localized at the Mg atoms nearby. However, electron accumulation and depletion are both

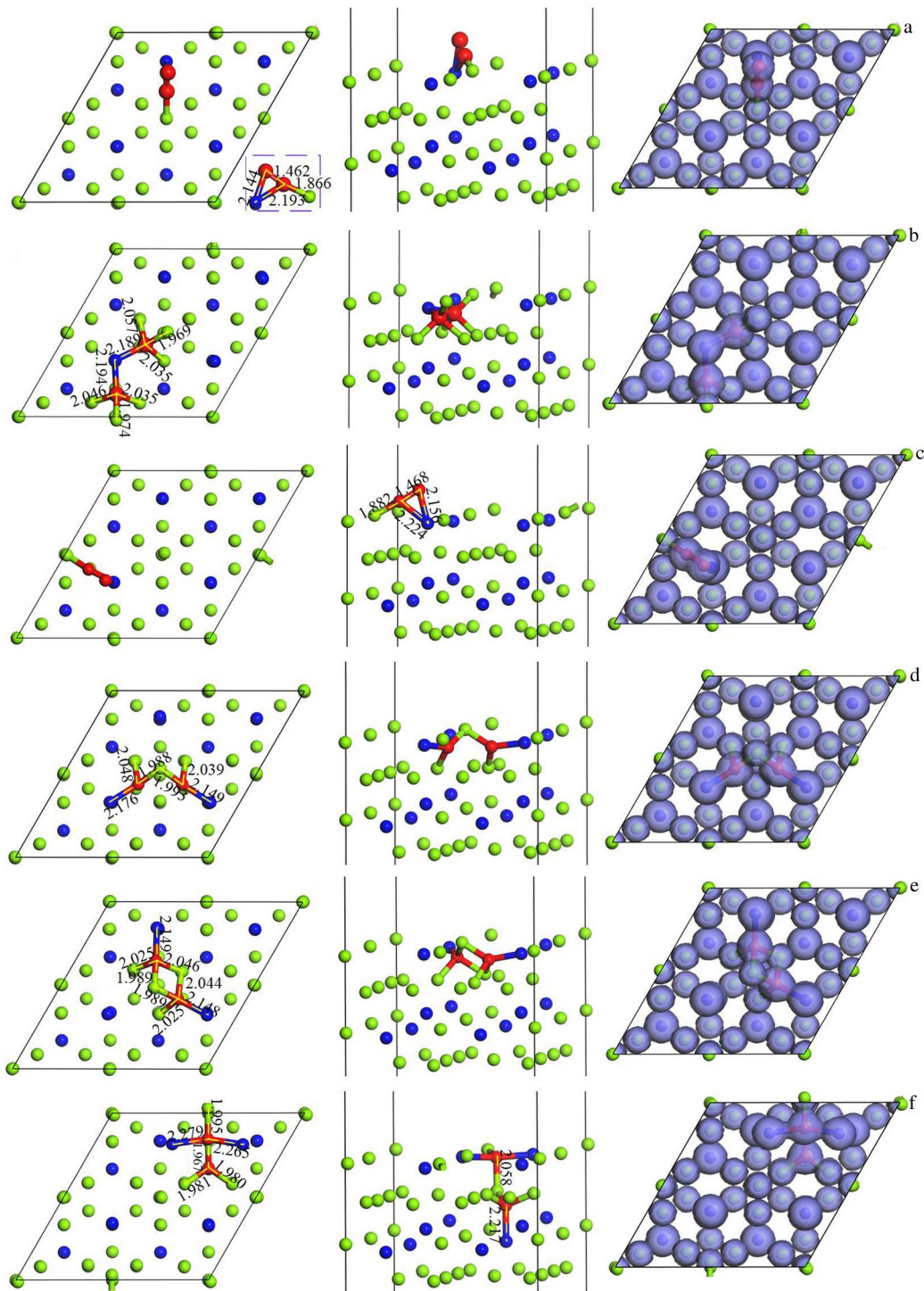


Fig.9 Adsorption configurations and parameters for adsorption system of Mg_2Ca : (a) site ①, (b) site ②, (c) site ③, (d) site ④, (e) site ⑤, and (f) site ⑥

localized at the Ca atom, and electron deletion mainly exists along the Ca-O bond. Combined with the Hirshfeld analysis tabulated in Table 1, O atoms obtain electrons and Mg atoms lose electrons. Although electron accumulation and deletion are both localized at the Ca atom, the Hirshfeld charge demonstrates that Ca atom loses electrons finally. Hence, during the adsorption, Mg_2Ca donates electrons to O_2 .

The transfer charges of O atoms in each adsorption system are -0.674, -0.920, -0.671, -0.901, -0.924, and -0.900 e. It is noteworthy that site ⑤ shows the highest charge transfer value, illustrating the most strong adsorption. For site ① and ③, the low charge transfer values illuminate the poor adsorption. The results are consistent with the E_{ad} values analysis. Nevertheless, compared with the charge transfer values in O_2 adsorption on $\alpha\text{-Mg}$, charge transfer values in O_2

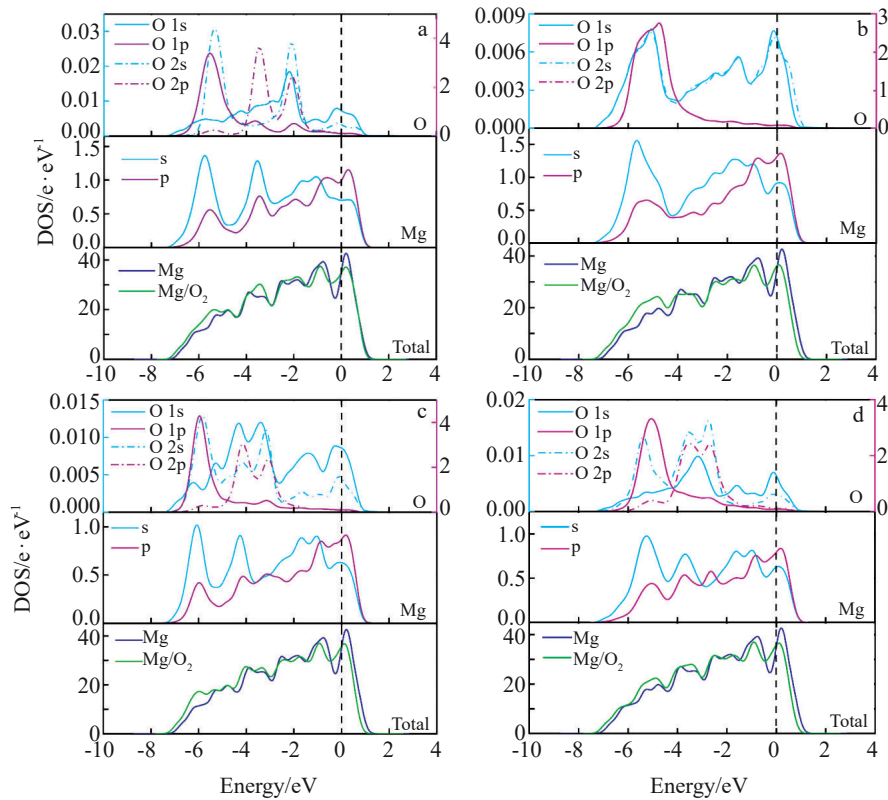


Fig.10 DOS distributions of adsorption systems on Mg: (a) site ①, (b) site ②, (c) site ③, and (d) site ④

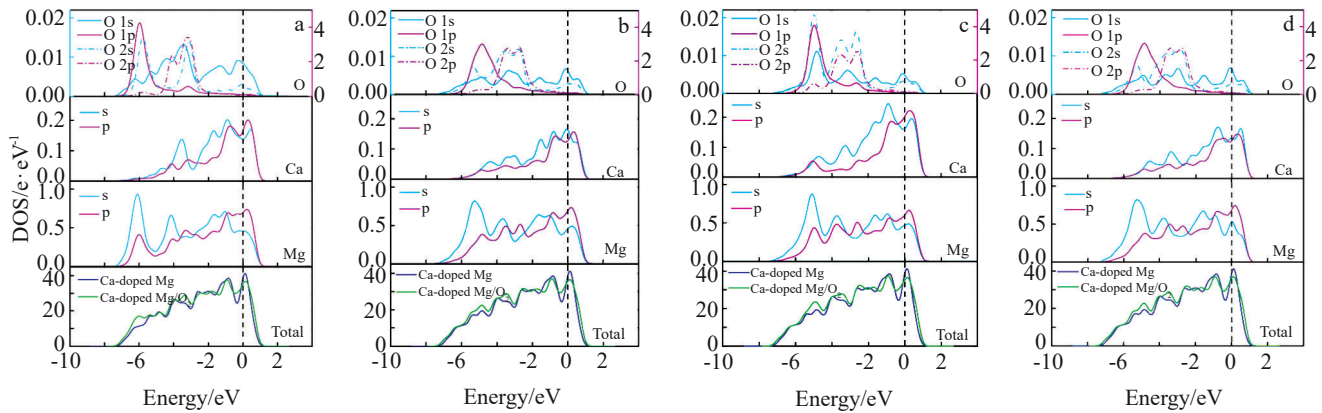


Fig.11 DOS distributions of adsorption systems on α -Mg: (a) site ①, (b) site ②, (c) site ③, and (d) site ④

adsorption on Mg_2Ca are lower, indicating that the adsorption structures of Mg_2Ca adsorption systems are less stable than those of α -Mg adsorption systems. That is, the Mg-Ca-O formed on Mg_2Ca is not as stable as that formed on α -Mg. The results are consistent with the adsorption structure analysis above, in which unbroken O-O bond exists in Mg_2Ca adsorption systems, while previous study showed that O-O bond suffers breakage in α -Mg adsorption systems.

Generally, the strong electron accumulation and electron depletion localized on the novel formed bonds manifest the strong electron hybridization^[40], which is in line with the Mg-O bond and Ca-O bond in this study.

2.4 Oxidation mechanism

During the adsorption of O_2 , O_2 tends to react with Ca, and adsorption structure containing Ca, Mg and O is formed, which is more stable than the adsorption structure containing O and Mg on Mg adsorption systems.

As shown in Fig.16, during the oxidation of α -Mg, O_2 preferentially reacts with the Ca in α -Mg to form the structure that contains Ca, Mg and O. Meanwhile, Ca atoms near the surface continuously diffuse to the surface to react with O_2 , and finally the structure covers the surface to form a Mg-Ca-O oxide film, which is more stable than MgO and can protect the substrate from

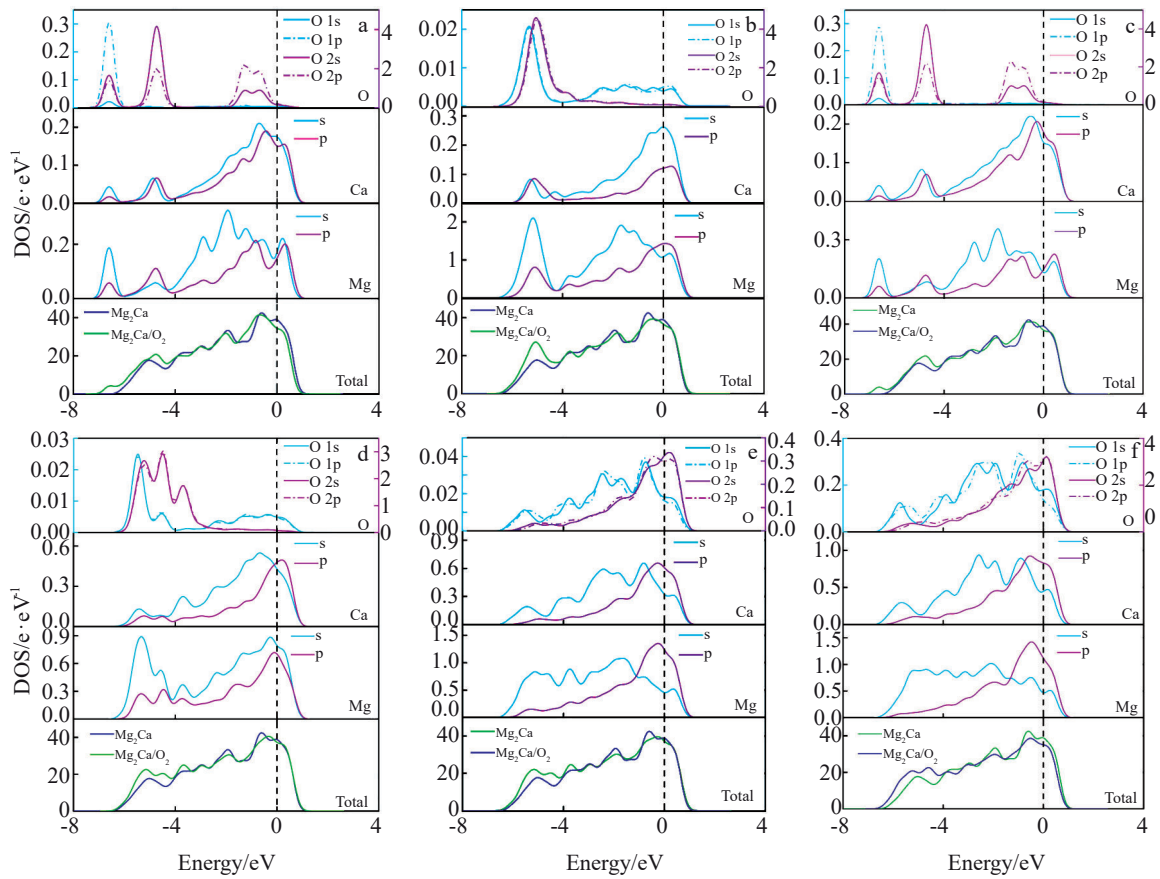


Fig.12 DOS distributions of adsorption systems on Mg_2Ca : (a) site ①, (b) site ②, (c) site ③, (d) site ④, (e) site ⑤, and (f) site ⑥

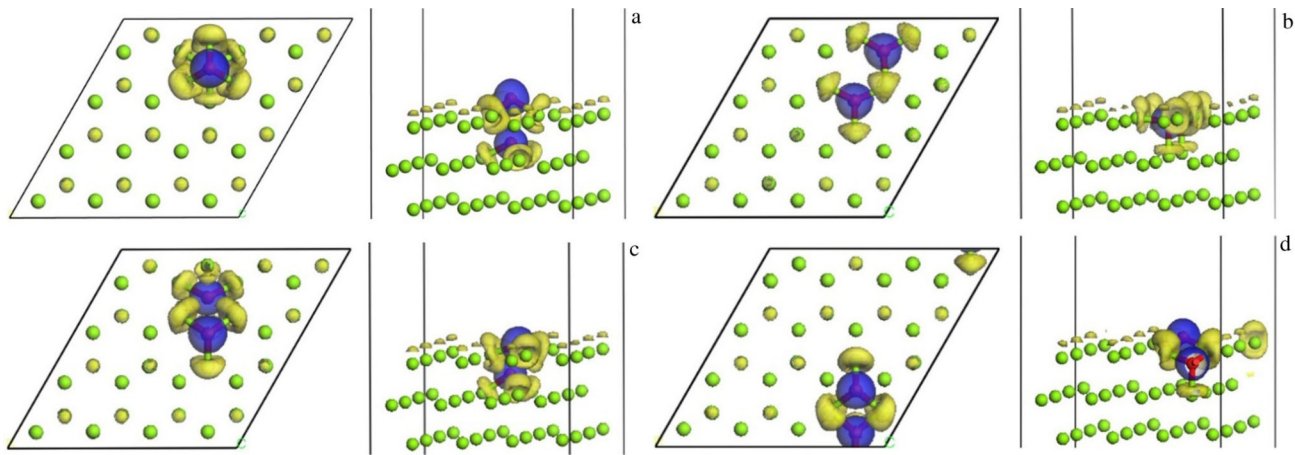


Fig.13 Electron density difference of Mg adsorption systems: (a) site ①, (b) site ②, (c) site ③, and (d) site ④

oxidation, thereby improving the oxidation resistance of the Mg_2Ca alloy.

The oxidation model of Mg_2Ca is described in Fig. 17. During the oxidation, O_2 reacts with the Ca and Mg in Mg_2Ca to form the structure containing Ca, Mg and O. Meanwhile, Ca atoms and Mg atoms near the surface continuously diffuse to the surface to react with O_2 , and finally the structure covers the surface to form $\text{Mg}_2\text{Ca-O}$

oxide film. Although $\text{Mg}_2\text{Ca-O}$ is formed on the surface to protect the substrate, the structure is not as stable as the structure formed on $\alpha\text{-Mg}$. Thus, the $\text{Mg}_2\text{Ca-O}$ oxide film formed on Mg_2Ca has less protective effect on substrate than the oxide film formed on $\alpha\text{-Mg}$. That is, Mg_2Ca shows limited protection to the oxidation of Mg_2Ca alloy.

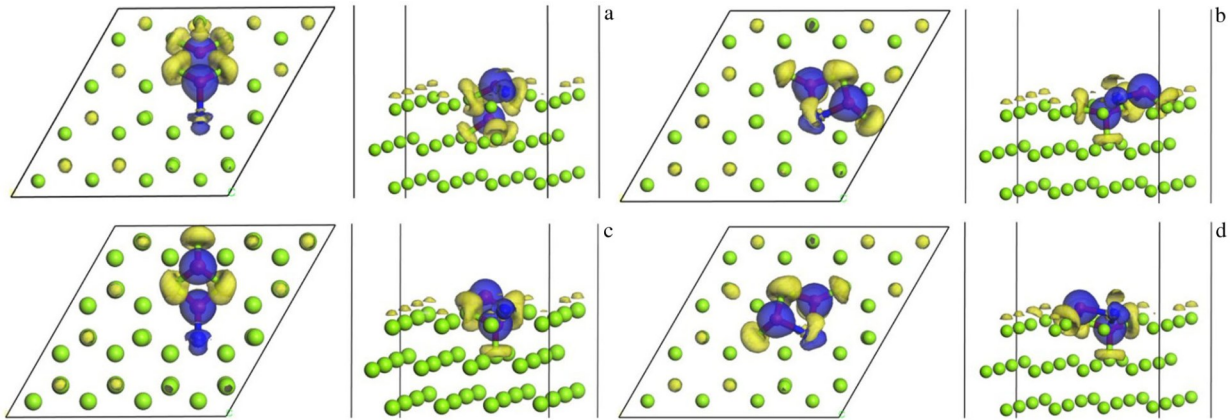
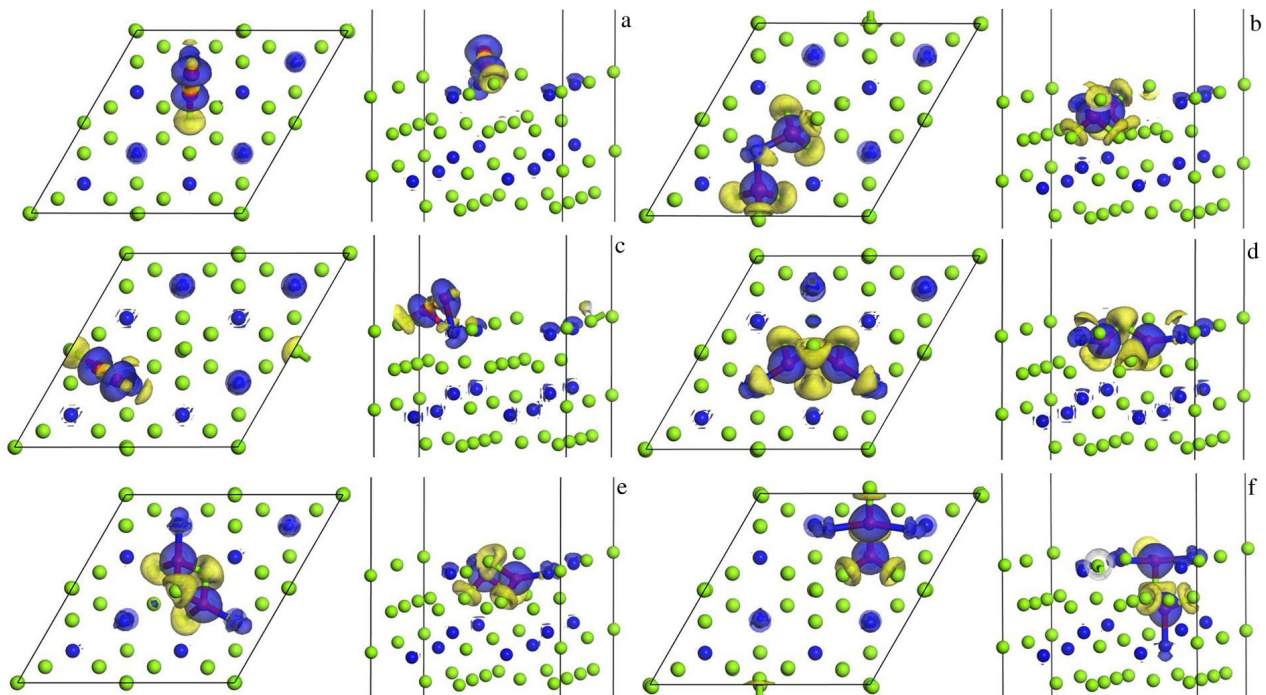
Fig.14 Electron density difference of α -Mg adsorption systems: (a) site ①, (b) site ②, (c) site ③, and (d) site ④Fig.15 Electron density difference of Mg_2Ca adsorption systems: (a) site ①, (b) site ②, (c) site ③, (d) site ④, (e) site ⑤, and (f) site ⑥

Table 1 Hirshfeld charge of adsorption systems

Substrate	Adsorption site	Hirshfeld charge/e			
		O1	O2	Bonding Mg	Ca
Mg	①	-0.383	-0.511	0.801	-
	②	-0.434	-0.434	0.929	-
	③	-0.375	-0.485	0.659	-
	④	-0.431	-0.500	0.827	-
α -Mg	①	-0.378	-0.517	0.514	0.230
	②	-0.449	-0.516	0.587	0.302
	③	-0.456	-0.501	0.676	0.227
	④	-0.449	-0.516	0.591	0.306
Mg_2Ca	①	-0.328	-0.346	0.167	0.172
	②	-0.459	-0.461	0.544	0.366
	③	-0.313	-0.358	0.131	0.199
	④	-0.450	-0.451	0.320	0.487
	⑤	-0.462	-0.462	0.556	0.238
	⑥	-0.427	-0.471	0.422	0.506

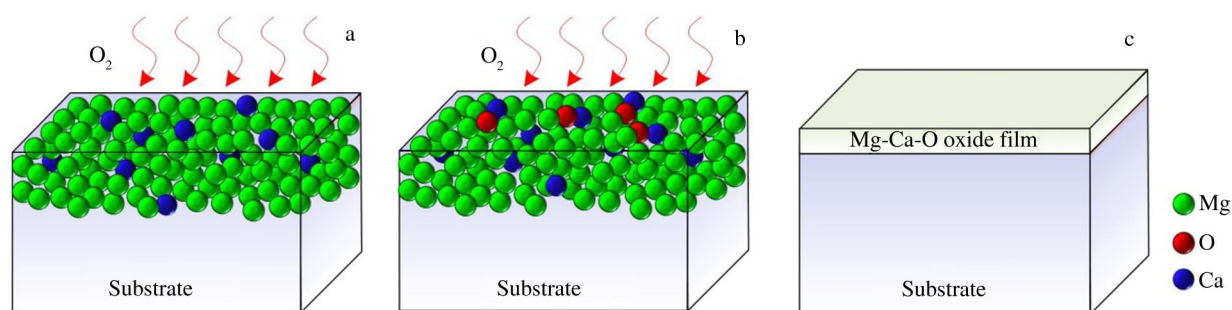


Fig.16 Oxidation model of α -Mg in Mg-Ca alloy: (a) before oxidation, (b) during oxidation, and (c) after oxidation

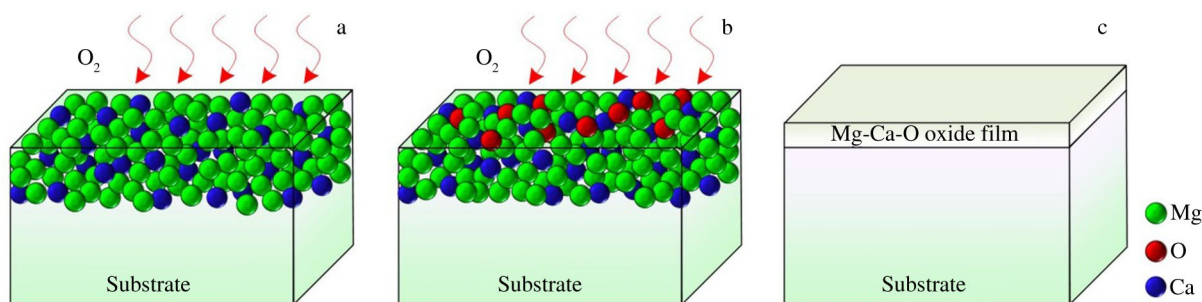


Fig.17 Oxidation model of Mg_2Ca in Mg-Ca alloy: (a) before oxidation, (b) during oxidation, and (c) after oxidation

3 Conclusions

1) During the adsorption on Mg, O atoms migrate to Mg atoms nearby. However, during the adsorption on α -Mg and Mg_2Ca , O tends to migrate to Ca.

2) These adsorptions are assumed to be chemisorption due to the remarkable E_{ad} values. α -Mg adsorption systems possess more desirable adsorption performances with more stable adsorption structures than Mg adsorption systems, and the adsorption structures in Mg_2Ca adsorption systems are not as stable as those in α -Mg.

3) During the oxidation of Mg-Ca alloy, O_2 is more likely to react with Ca atoms rather than Mg atoms. Hence a stable Mg-Ca-O oxide film is formed to improve the oxidation resistance of Mg-Ca alloy. However, the Mg-Ca-O oxide film formed on Mg_2Ca is not as stable as that on α -Mg. That is, Mg_2Ca shows limited protection to the oxidation of Mg-Ca alloy.

References

- Yang L, Yuan Y, Chen T et al. *Intermetallics*[J], 2017, 133: 107 171
- Che X, Wang Q, Dong B B et al. *Journal of Magnesium Alloys* [J], 2021, 9(5): 1677
- Xu T C, Yang Y, Peng X D et al. *Journal of Magnesium Alloys* [J], 2019, 7(3): 536
- Zhang J L, Huang Y, Xiang J et al. *Materials Science and Engineering A*[J], 2021, 800: 140 320
- Wei Y K, Li Y J, Zhang Y et al. *Corrosion Science*[J], 2018, 138: 105
- Chen H K, Jiang H L. *Corrosion Science*[J], 2021, 179: 109 148
- Chen H K, Jie Y Y, Chang L et al. *Solid State Ionics*[J], 2019, 340: 11 501
- Tan Q Y, Atrons A, Mo N et al. *Corrosion Science*[J], 2016, 112: 734
- Tan Q Y, Yin Y, Mo N et al. *Surface Innovations*[J], 2019: 1
- Inoue S, Yamasaki M, Kawamura Y. *Corrosion Science*[J], 2020, 174: 108 858
- Inoue S, Yamasaki M, Kawamura Y. *Corrosion Science*[J], 2019, 149: 133
- Tan Q Y, Mo N, Lin C L et al. *Corrosion Science*[J], 2018, 132: 272
- Yu X W, Jiang B, He J J et al. *Journal of Alloys and Compound* [J], 2018, 749: 1054
- Zeng R C, Qi W C, Cui H Z et al. *Corrosion Science*[J], 2015, 96: 23
- Pan H C, Qin G W, Ren Y P et al. *Journal of Alloys and Compound*[J], 2015, 630: 272
- Lee T W, Park H W, Lim H et al. *Journal of Alloys and Compound*[J], 2017, 714: 397
- Lee D B. *Oxidation of Metals*[J], 2016, 85(1-2): 65
- Cheng C L, Lan Q, Wang A et al. *Metals*[J], 2018, 8: 766
- Paridari S, Larijani H S, Ghasem E B. 2018: *Magnesium Technology*[C]. Pennsylvania: TMS, 2018: 297
- Li F, Peh W Y, Nagarajan V et al. *Materials & Design*[J], 2016, 99: 37
- You B S, Park W W, Chung I S. *Scripta Materialia*[J], 2000, 42(11): 1089
- Yuasa M, Hayashi M, Mabuchi M, et al. *Acta Materialia*[J], 2014, 65: 207

- 23 Hu H, Zhang Q, Niu X P. *Defect and Diffusion Forum*[J], 2011, 312-315: 271
- 24 Zhou Y J. *Thesis for Doctorate*[D]. Harbin: Harbin Institute of Technology, 2014: 29 (in Chinese)
- 25 Fang Z, Wang J F, Yang X F et al. *Applied Surface Science*[J], 2017, 409: 149
- 26 Dong J L, Gao Z Y, Yang W J et al. *Applied Surface Science*[J], 2019, 480: 779
- 27 Cui H, Zhu H L, Jia P F. *Applied Surface Science*[J], 2020, 530: 14 724
- 28 Lee Y, Lee S, Hwang Y et al. *Applied Surface Science*[J], 2014, 289: 445
- 29 Mukherjee S, Banwait A, Grixti S et al. *ACS Applied Materials & Interfaces*[J], 2018, 6: 5373
- 30 Kumar A, Ropital F, Bruin T D et al. *Applied Surface Science*[J], 2020, 529: 147 127
- 31 Mofidi F, Reisi-Vanani A. *Applied Surface Science*[J], 2019, 507: 145 134
- 32 Zhang X X, Zhang J, Cui H. *Journal of Fluorine Chemistry*[J], 2018, 213: 18
- 33 Cui H, Jia P F, Peng X Y. *Applied Surface Science*[J], 2020, 513: 145 863
- 34 Gui Y G, Li W J, He X et al. *Applied Surface Science*[J], 2020, 507: 145 163
- 35 Gao X, Zhou Q, Wang J X et al. *Applied Surface Science*[J], 2020, 517: 146 180
- 36 Ma D W, Ma B Y, Lu Z W et al. *Physical Chemistry Chemical Physics*[J], 2017, 19: 26 022
- 37 Cortés-Arriagada D, Villegas-Escobar N. *Applied Surface Science*[J], 2017, 420: 446
- 38 Zhang T, Sun H, Wang F D et al. *Applied Surface Science*[J], 2017, 425: 340
- 39 Cui H, Jia P F, Peng X Y et al. *Materials Chemistry and Physics* [J], 2020, 249: 123 006
- 40 Cui H, Yan C, Jia P F et al. *Applied Surface Science*[J], 2020, 512: 145 759

从吸附角度观察 Mg-Ca 合金中 Mg_2Ca 和 $\alpha\text{-Mg}$ 的氧化: DFT 研究

明 玥¹, 游国强^{1,2}, 彭力真¹, 张 军³, 曾 文¹, 赵建华^{1,2}

(1. 重庆大学 材料科学与工程学院, 重庆 400044)

(2. 重庆大学 国家镁合金材料工程技术研究中心, 重庆 400030)

(3. 慕尼黑工业大学, 德国 慕尼黑 80333)

摘 要: 基于 DFT 计算 O_2 在 $\alpha\text{-Mg}$ (0001) 和 Mg_2Ca (0001) 上的吸附过程, 以探明 Mg-Ca 合金中的 $\alpha\text{-Mg}$ 和 Mg_2Ca 氧化机理。结果表明, 在吸附过程中, O_2 与 $\alpha\text{-Mg}$ 和 Mg_2Ca 有很强的相互作用, 且均为化学吸附, 但 Mg_2Ca 的吸附结构不如 $\alpha\text{-Mg}$ 的吸附结构稳定。在氧化过程中, O_2 与 $\alpha\text{-Mg}$ 和 Mg_2Ca 中的 Ca 和 Mg 原子发生反应, 形成 Mg-Ca-O 氧化膜, 从而提高 Mg-Ca 合金的抗氧化性。但 Mg_2Ca 的吸附结构稳定性比 $\alpha\text{-Mg}$ 差, 因此 Mg_2Ca 形成的氧化膜对基体的保护作用比 $\alpha\text{-Mg}$ 弱。

关键词: Mg_2Ca ; $\alpha\text{-Mg}$; 氧化; 密度泛函理论

作者简介: 明 玥, 女, 1990 年生, 博士, 重庆大学材料科学与工程学院, 重庆 400044, E-mail: ming0717yue@163.com